SS-HCNN: Semi-Supervised Hierarchical Convolutional Neural Network for Image Classification

Tao Chen, Shijian Lu, and Jiayuan Fan

***Abstract*— The availability of large-scale annotated data and the uneven separability of different data categories have become two major impediments of deep learning for image classification. In this paper, we present a semi-supervised hierarchical convolutional neural network (SS-HCNN) to address these two challenges. A large-scale unsupervised maximum margin clustering technique is designed, which splits images into a number of hierarchical clusters iteratively to learn cluster-level CNNs at parent nodes and category-level CNNs at leaf nodes. The splitting uses the similarity of CNN features to group visually similar images into the same cluster, which relieves the uneven data separability constraint. With the hierarchical cluster-level CNNs capturing certain high-level image category information, the category-level CNNs can be trained with a small amount of labeled images, and this relieves the data annotation constraint. A novel cluster splitting criterion is also designed, which automatically terminates the image clustering in the tree hierarchy. The proposed SS-HCNN has been evaluated on the CIFAR-100 and ImageNet classification datasets. The experiments show that the SS-HCNN trained using a portion of labeled training images can achieve comparable performance with other fully trained CNNs using all labeled images. Additionally, the SS-HCNN trained using all labeled images clearly outperforms other fully trained CNNs.**

***Index Terms*— SS-HCNN, semi-supervised, hierarchical, unsupervised, image classification.**

I. Introduction

THE deep convolutional neural network (CNN) has been developed in various image classification applications [1]–[8]. On the other hand, the deployment of deep CNN is facing two critical challenges: annotation of large-scale image datasets and uneven image separability across different object categories, e.g., "dog" and "sheep" images share higher visual similarity and are more difficult to separate, whereas "person" and "car" images share lower visual similarity and are much easier to differentiate. The traditional flat N-way CNN [1], [2] does not consider such uneven separability and often leads to sub-optimal object classification performance.

We propose a Semi-Supervised Hierarchical Convolutional Neural Network (SS-HCNN) that aims to address the image annotation constraint and category-wise uneven separability challenge. The idea is to partition images into a hierarchy of clusters through unsupervised clustering of the low-level features, and accordingly train a hierarchy of CNNs at root and parent nodes by using the generated cluster labels. The clusters at leaf nodes are more compact and consist of visually similar images of a small number of object categories, where CNNs can be trained effectively by using a small amount of image annotations. The SS-HCNN therefore consists of two training stages. The first is unsupervised which iteratively partitions images into clusters through clustering of the low-level image features and trains CNNs at root and parent nodes by using the generated cluster labels as the ground truth. The clustering process is iterative and terminates automatically according to a defined criterion. It relieves the uneven image separability constraint by clustering visually similar images into the same cluster where dedicated CNN can be trained for better classification performance. The second is supervised which trains category-level CNNs at leaf nodes for discriminative image classification. As the CNNs at parent nodes perform certain high-level coarse classification of images, the leaf node clusters are more compact and consist of images of a much smaller number of categories as compared with the original image set. Therefore, the category-level CNNs can be trained using a small amount of labelled training images and this relieves the data annotation challenge greatly.

The contributions of this work are threefold. First, it proposes a two-stage semi-supervised CNN learning framework that addresses the uneven image separability and image annotation constraints simultaneously, and demonstrates its superior performance in different image classification tasks. Second, it proposes a large-scale unsupervised maximum margin clustering technique that employs the minibatch strategy to cluster the fully connected (FC) image features for hierarchical cluster-level CNN learning. Third, it designs a novel cluster splitting criterion which terminates the hierarchical clustering process automatically based on the underlying visual and structural image similarity. A voting based image scoring function is designed which classifies images by combining output of an ensemble of multiple leaf node CNNs.

Manuscript received January 31, 2018; revised October 25, 2018; accepted December 1, 2018. Date of publication December 14, 2018; date of current version January 30, 2019. The associate editor coordinating the review of this manuscript and approving it for publication was Dr. Liang Wang. *(Corresponding author: Jiayuan Fan.)*

T. Chen is with the School of Information Science and Technology, Fudan University, Shanghai 200433, China (e-mail: ntuchentao@gmail.com).

S. Lu is with the School of Computer Science and Engineering, Nanyang Technological University, Singapore 639798 (e-mail: shijian.lu@ntu.edu.sg).

J. Fan is with the Satellite Department, Institute for Infocomm Research, Singapore 138632 (e-mail: fanj@i2r.a-star.edu.sg).

Digital Object Identifier 10.1109/TIP.2018.2886758

II. Related Works

A. Semi-Supervised CNN Learning

Due to the challenges in collecting large-scale datasets and manual data annotation, semi-supervised CNN learning that uses partially labelled data samples has attracted increasing interest in recent years [4], [9]–[13]. Sparse Laplacian filter learning is adopted to obtain the network filters with unlabelled data for vehicle type classification [4]. In [9], a semi-supervised regularizer is added in the hidden or output loss layer or another separate auxiliary network sharing the first several layers with the original CNN in the deep structure. In [10] and [11], they combine text region embeddings of variable sizes in the form of Long Short-Term Memory (LSTM) and convolution layers trained on the unlabelled data for text categorization. In [12], an online Expectation-Maximization (EM) method is developed to train deep CNN models from weakly annotated data. The method alternates between estimating the latent pixel labels and optimizing the DCNN parameters using stochastic gradient descent (SGD). In [13], an interesting model is proposed which first uses random noise to supervise the CNN pre-training and then learns CNN features through stochastic gradient descent (SGD) in an unsupervised manner. A common constraint of these works is that they adopt the flat N-way CNN as the learning structure where the uneven data separability problem is not well addressed.

B. Hierarchical CNN Learning

Several hierarchical learning methods have also been developed in recent years to address the uneven data separability problem [14]–[19]. In [14], the label relationships are encoded in a hierarchical tree to improve the object classification accuracy. In [15], a hierarchy of CNNs is introduced with only two coarse categories due to the scalability issue. The work [16] builds a hierarchical CNN with the main objective of transferring knowledge from a large network to a small network to achieve scalability. In [17], a two-level hierarchical CNN is designed to separate easy classes using a coarse category classifier and difficult classes using fine category classifiers. In [18], a multi-level deep decision neural network is built where each node in the tree is a CNN. In [19], a two-level tree-structured network architecture is designed, which contains a generalist network producing coarse grouping of classes, and a set of expert networks for recognition of classes within each group. Crucially, the partition of categories is learned simultaneously with the parameters of the network trunk and the experts are trained jointly by minimizing a single learning objective over all classes.

These hierarchical CNN methods suffer from three typical limitations. First, they identify the image category hierarchy by performing spectral clustering on category confusion matrix [14]–[18], which is fully supervised requiring annotations of all training images. Second, they perform category-level clustering by grouping several fine image categories into a single coarse image category [14]–[19], which will introduce larger variations. In addition, the clustering from fine categories into coarse categories may lead to misclassification of test images once they are classified into an incorrect coarse category at the beginning. Third, they either manually specify the depth of the hierarchy tree [17] or terminate the clustering according to the validation performance [18], and produce a flat tree where all the leaf nodes have the same depth. This ignores the fact that different clusters have different diversity and should be split into leaf nodes of different granularities and depth.

The proposed SS-HCNN addresses the above-mentioned constraints from several aspects. First, it adopts a hierarchical structure and mitigates the uneven data separability problem effectively. Second, the SS-HCNN performs unsupervised image clustering based on the underlying image feature similarity without requiring image labels. With the learned cluster-level CNNs at parent nodes which perform certain high-level classification tasks, only a small amount of labelled images are needed to train the category-level CNNs at leaf nodes. Third, instead of clustering based on image labels as in [17] and [18], the SS-HCNN clusters images based on the underlying image feature similarity where images of the same object category may be clustered into different coarse categories. As a result, the risk of classifying a test image into an incorrect coarse category at the early stage is reduced because different coarse categories (clusters) under SS-HCNN may contain images of the same object category. Finally, the SS-HCNN designs an automatic and adaptive cluster splitting mechanism to address the image uneven separability issue. According to the underlying image feature similarity, the SS-HCNN clustering will stop early for images with high separability, e.g. "people" and "car" images, but continues to deeper layers for images with lower separability, e.g. "dog" and "sheep" images.

III. The Proposed Method

A. SS-HCNN Overview

The SS-HCNN is a tree structured deep hierarchical CNN, where each parent node corresponds to a cluster-level CNN which is trained through unsupervised clustering, and each leaf node corresponds to a category-level CNN which is trained through supervised learning. Fig. 1 shows an overview of the SS-HCNN layer structure and image clustering process at different nodes. A pre-trained CNN model such as VGG [2] or ResNet [3] is first employed as the root node CNN to extract the fully connected (FC) features from each training image. The extracted FC features are then partitioned into multiple clusters through maximum margin clustering (MMC) [20] which assigns a cluster label to each training image. To avoid the time-consuming MMC clustering process while classifying a test image, a new softmax layer (red bar in Fig. 1) is added to train the root CNN to learn the correlation between each FC feature vector and the corresponding cluster label as generated by MMC. Therefore, the fine-tuning of the root node CNN (from the initial pre-trained CNN model) is unsupervised which uses the MMC-generated cluster labels as ground-truth labels. During the testing stage, the fine-tuned root node CNN can thus predict a cluster label for each test image as indicated by the red dotted line in Fig. 1.

Note that using a pre-trained model is a widely adopted transfer learning practice since networks trained using

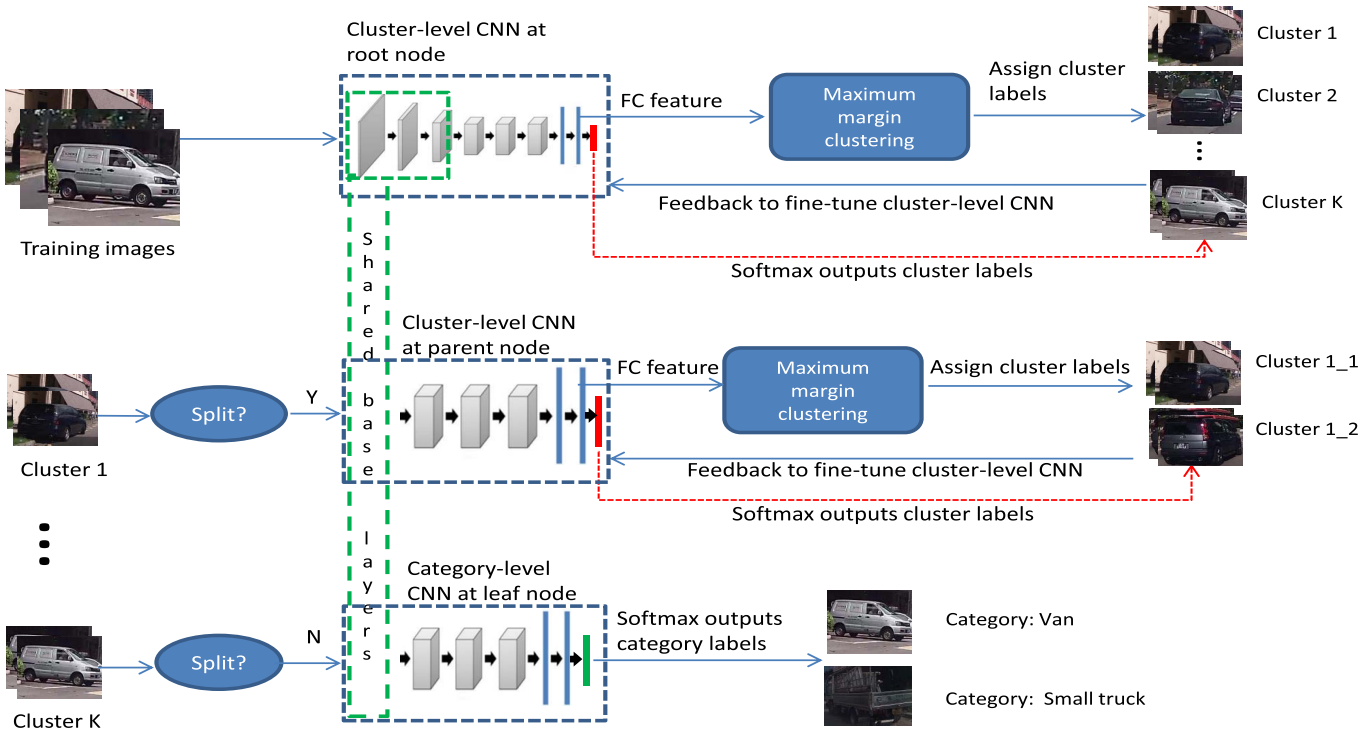

Fig. 1. Overview of the image clustering and CNN training process at different nodes in the proposed tree structured SS-HCNN.

different image datasets usually have similar lower layers which largely capture low-level features such as edges and corners [18], [21], [22]. In the SS-HCNN, we borrow the lower layers of a pre-trained CNN model to extract convolutional features for MMC. The MMC-produced cluster labels are then used as the ground truth to fine-tune the pre-trained CNN model so that it can produce consistent label predictions while classifying a new image during the testing phase.

A splitting criterion is designed to control the splitting of all clusters as generated by the root node, i.e. Cluster 1, Cluster 2, . . . ,Cluster K as shown in Fig. 1. If further splitting is needed, each generated cluster will go through the same MMC clustering and CNN fine-tuning process as the root node, which further produces child clusters, e.g., Cluster 1_1, Cluster 1_2 as illustrated in Fig. 1. Otherwise, the current cluster, e.g. Cluster K in Fig. 1, becomes a leaf cluster which contains images that have similar appearance, much smaller feature divergence and a much smaller number of image categories as compared with the original image dataset. A category-level CNN is finally trained by using a certain portion of leaf cluster images together with their annotations, where a new softmax layer (green bar in Fig. 1) is added for training. It is usually more accurate and reliable when a larger portion of the leaf cluster images together with their annotations are used for training. During the testing phase, the category-level CNN at a leaf node will predict a category label for each test image that is routed to that leaf node.

B. Large-Scale Unsupervised Hierarchy Learning

The purpose of learning a CNN hierarchy is two folds. First, it targets to group visually similar images of different categories into the same coarse cluster and train dedicated cluster-level CNNs for better classification of the clustered images, hence addresses the uneven image separability effectively. Second, it trains a set of cluster-level CNNs that can perform high-level classification of test images. As a result, only a small amount of annotated images are needed to train the category-level CNNs at leaf nodes which relieves the image annotation challenge greatly.

We derive the image cluster labels by employing the MMC [20] which is an extension of the supervised large margin theory to the unsupervised scenario. The MMC optimizes the linear models learned for each cluster and simultaneously classifies each sample into a cluster, often leading to more compact clusters than other graph or spectral based methods [17], [23]. The superiority of MMC over traditional clustering methods such as k-means has also been reported extensively in earlier works [20], [24]. On the other hand, the original MMC is more suitable for small-scale data clustering due to the large margin optimization. We propose a large-scale MMC technique by incorporating the minibatch idea that is widely used in CNN training [1] as described below.

Suppose $\{\mathbf{f}_i\}_{i=1}^{M}$ denote the FC feature vectors extracted from the first minibatch of training images, where M is the minibatch size which is experimentally set at 1024, according to the compromise between the clustering speed and clustering accuracy. The MMC first identifies K clusters from the M feature vectors by solving the following objective function,

$$\min_{W,Y,\xi\geq 0} \left\{ \frac{1}{2}\sum_{k=1}^{K} \|\mathbf{w}_k\|^2 + \frac{C}{K}\sum_{i=1}^{M}\sum_{j=1}^{K}\xi_{ij} \right\} \tag{1}$$

$$s.t.\ \sum_{k=1}^{K} y_{ik}\mathbf{w}_k^T\mathbf{f}_i - \mathbf{w}_j^T\mathbf{f}_i \geq 1 - y_{ij} - \xi_{ij}, \quad \forall i, j$$
$$y_{ik} \in \{0,1\}, \sum_{k=1}^{K} y_{ik} = 1 \quad \forall i, k$$
$$L \leq \sum_{i=1}^{M} y_{ik} \leq U, \quad \forall k \tag{2}$$

where $W = \{\mathbf{w}_k\}, k = 1, \ldots, K$ are the learned optimal linear models for the K clusters. The $Y = \{y_{ik}\}, i = 1, \ldots, M, k = 1, \ldots, K$ are the assigned cluster labels, where $y_{ik} = 1$ indicates that the i-th training sample is clustered into the k-th cluster. The $\xi = \{\xi_{ij}\}, i = 1, \ldots, M, j = 1, \ldots, K$ are slack variables to allow soft margin, and C is a trade-off parameter. The second constraint in Eq. 2 ensures that each training sample will be clustered into only one cluster. The last constraint controls the sample size of the k-th cluster to be between a lower bound L and an upper bound U, which generates a set of balanced clusters with moderate sample size. The parameters L and U are set at $0.9\frac{M}{K}$ and $1.1\frac{M}{K}$ respectively, by grid search that varies the multiplier coefficient between 0 and 2 with a step size of 0.1.

The second minibatch is then clustered into K clusters by MMC in the similar way. We merge each newly generated cluster with one of the K clusters as generated from the first minibatch based on the cluster similarity. In particular, the cluster similarity is computed by a matching score s_{kj} between each newly generated cluster j and previously generated cluster k as follows:

$$s_{kj} = \frac{1}{N_j}\sum_{i=1}^{N_j} \mathbf{w}_k^T\mathbf{f}_i \tag{3}$$

where N_j is a sample number of the newly generated cluster j, and $\mathbf{f}_i$ is the i-th feature vector within it. It can be seen that the matching score is computed by the average likelihood score of the FC feature vector $\mathbf{f}_i$ in the newly generated cluster j as evaluated by the previously trained cluster model $\mathbf{w}_k$. The newly generated cluster j is thus merged into the previously generated cluster k that produces the largest matching score s_{kj} as defined in Eq. 3.

The merged cluster acts as the new cluster k for the merging of the later clusters. To avoid the complex cluster model re-training, we keep both linear models $\mathbf{w}_k$ and $\mathbf{w}_j$ from clusters k and j and use an ensemble of the two component models for merging newly generated clusters. From the third image minibatch onwards, the matching score s_{kj} will thus be computed as follows:

$$s_{kj} = \frac{1}{N_j}\sum_{i=1}^{N_j}\left(\max_{p=1,\ldots,P}\left(\mathbf{w}_p^T f_i\right)\right) \tag{4}$$

where P is the number of the accumulated component models in the merged cluster k. It can be seen that the maximum matching score across the ensemble component models is used to decide the merging of the new clusters as generated from the third minimatch and thereafter. At the end, each new cluster as generated from the ensuing image minibatches is linked to one of the previous K clusters as defined in Eq. 4, and all images in the large-scale dataset will be assigned with a cluster label. These cluster labels will be used as the ground truth to fine tune the cluster-level CNNs, to be detailed in Section 3.4.

For clustering of FC features extracted from large-scale datasets, the proposed minibatch based MMC is advantageous due to its high computational efficiency and manageability. As a comparison, global clustering such as k-means clustering is much more challenging because it is memory inefficient and computationally expensive - imagine loading million-scale vectors with each vector of thousands dimension into the memory and doing k-means on them. Additionally, global clustering is more liable to produce unbalanced clusters with very large or small sizes. The minibatch based MMC clustering aims to capture the overall underlying image similarity which may not always cluster an image into the correct cluster. On the other hand, it will always route an image to one leaf node cluster where the image category information will be captured by the category-level CNN. Given a new test image, we also design an image scoring scheme which combines outputs of multiple leaf-node CNNs to address the possible image mis-clustering problem (more details to be presented in Section 3.5).

Note that unlike flat CNNs such as [13], updating clusters during the CNN fine-tuning does not introduce much change to the clusters in SS-HCNN. To verify this, we conducted a new test by updating clusters while fine-tuning the cluster-level CNN, and the study shows that the clusters have little change throughout the iterative CNN fine-tuning process. The little cluster change is largely due to two reasons: 1) the cluster-level CNN in SS-HCNN is pre-trained using correct category labels, which has better cluster prediction capability than [13] that starts with random noise for supervision of the CNN pre-training; 2) SS-HCNN adopts a hierarchical structure where cluster-level CNN only predicts 3 or 4 (for CIFAR or ImageNet to be discussed later) cluster labels which are very coarse categorization and less prone to errors, whereas flat CNNs such as [13] predict a much larger number of fine categories.

C. Cluster Splitting

Determining when to stop cluster splitting is important to control the depth of the tree-structured CNN hierarchy. Over-splitting of a cluster brings little accuracy gain but increases computational costs greatly. We design a cluster splitting metric that considers both the cluster size and the feature divergence as defined by,

$$d = \mathbf{I}\left(N_k > t\right) \cdot \log\left(\frac{\sum_{i=1}^{N_k}\left(\max_{p=1,\ldots,P}\left(\mathbf{w}_p^T f_i\right)\right)}{\sum_{i=1}^{N_k}\left(\min_{p=1,\ldots,P}\left(\mathbf{w}_p^T f_i\right)\right)}\right) \tag{5}$$

where d is the metric score which controls the clustering termination by comparing it with a pre-defined threshold. The $\mathbf{I}$ is an indicator function having the value of 1 when the cluster size N_k satisfies $N_k > t$ (t is a threshold) or 0 otherwise. It ensures that each cluster should have a sufficient number of

images for CNN training. The threshold t is set at 500 based on experiments which help to avoid CNN overfitting.

The log probability ratio in Eq. 5 denotes the divergence of the component cluster models in the merged cluster k. In particular, the numerator corresponds to the sum of the probability that the cluster images are generated by its most probable component cluster model, and the denominator corresponds to the sum of the probability that the cluster images are generated by its most unlikely component cluster model. If the values of the two are far from each other, the component cluster models in k are considered to have large divergence and splitting should continue. Otherwise the cluster splitting terminates and the current cluster becomes a leaf cluster. During the whole cluster splitting process, the algorithm discovers the image hierarchy automatically according to the image feature similarity, where no image category label information is required.

D. SS-HCNN Training

The proposed SS-HCNN trains a hierarchy of CNNs at root, cluster and category levels to address the data annotation and uneven separability constraints. One major issue in the SS-HCNN training is data imbalance where images in a minibatch may be routed to different clusters at different nodes. We address this issue by breaking the training into multiple phases instead of training as a whole. In particular, we first train the root node CNN which will serve as a basis for the subsequent training of cluster- and category-level CNNs at parent and leaf nodes.

The root node CNN is trained as shown in Fig. 1. With MMC-assigned cluster labels, the root CNN is fine tuned by setting the optimization objective as the cross entropy loss between the CNN-predicted cluster labels and the MMC-assigned cluster labels. Such cluster label based CNN training has two advantages. First, the base layers of the root node CNN can be shared with its child CNNs as they capture similar low-level features. The child CNNs can thus focus more on the training of their rear layers through clustering images in the corresponding clusters. Second, the computationally expensive MMC will not be required during the testing stage because the learned root-node CNN can predict a cluster label for each test image.

For cluster-level CNNs at parent nodes, the base layers are directly inherited from the base layers of their parent CNNs (at root node), and the deeper layers are fine-tuned by using the cluster labels that are obtained during the MMC clustering. The cluster labels thus provide supervision information in the similar way as annotation labels that are used in fully supervised training. For category-level CNNs at leaf nodes, the base layers are similarly inherited from the base layers of their parent CNNs with no modifications. The deep layers, which handle the image category classification directly, are fine-tuned by minimizing the cross entropy loss between the predicted category labels and the ground-truth category labels (different amounts of labeled images are used to train the leaf-node CNNs). Therefore, the major difference between the cluster-level CNN training (at parent nodes) and the category-level CNN training (at leaf nodes) is that cluster-level CNNs use the MMC generated cluster labels as the ground-truth whereas category-level CNNs use the annotated category labels as the ground-truth. Note that the image category distribution in different leaf-node clusters may be imbalanced which could introduce training bias. We address this issue by (i) sampling training images of different categories as uniform as possible for each training mini-batch, and (ii) performing data augmentation to generate more training samples for the image categories with much less samples.

E. SS-HCNN Testing

In the testing stage, a test image is first feedforwarded to the root node where the softmax layer will output a score vector a_k, $k = 1, \ldots, K$ indicating the probabilities of the image belonging to the K clusters. The child clusters where the test image will be routed to is determined based on the score ratio r as follows,

$$r = \frac{\max\limits_{k=1,\ldots,K} a_k}{\max\limits_{k=1,\ldots,K,k\neq j} a_k} \tag{6}$$

where j refers to the child cluster having the highest score.

We use the ratio between the highest and second highest score to select the child clusters as defined in Eq. 6. In particular, if the ratio r is larger than a threshold, the cluster j has high confidence of being the right cluster and it will be selected. Otherwise, the top two clusters have high chance as the right clusters and both are selected to maximize the probability of correct routing of the test image. In experiments, we change the threshold ratio from 0.1 to 2 with a step size of 0.1, and the best classification accuracy is achieved when the threshold is set at 1.3. We therefore set the threshold at 1.3.

The above process repeats until the test image is finally routed to one or multiple leaf node clusters. When the test image is routed to a single leaf node cluster, it is directly classified by the corresponding leaf node CNN. When the test image is routed to multiple leaf node clusters instead, it is classified by a voting strategy defined as follows,

$$y = \arg\max_{c=1,\ldots,C} \sum_{l=1}^{L} a_c^l \tag{7}$$

where y is the determined image category for the test image, a_c^l refers to the softmax output of the l-th leaf CNN for category c, C is the number of image categories and L is the number of the traversed leaf nodes by the test image. The image category that has the maximum total response across all the traversed leaf node CNNs is thus selected as the image's belonging category.

IV. Experiments

We evaluate the proposed SS-HCNN on CIFAR-100 [25] and ImageNet datasets [26]. CIFAR-100 is composed of 100 classes of natural images, including 50K training images and 10K testing images. ImageNet [26] consists of 1000 classes of natural images, including 1.2 million training images and 50,000 validation images. The SS-HCNN

is implemented on the Caffe [27] software. The system runs on a workstation with Intel core i7-5960X CPU 3.00GHz, NVIDIA GTX-Titan GPU, and 64GB RAM.

A. CIFAR-100

Setup: The CIFAR-100 dataset is similarly pre-processed using global contrast normalization and ZCA whitening [18]. The network in network (NIN) [5] is used as the CNN structure at each node in the proposed SS-HCNN. The original NIN consists of three MLP layers. The first two MLP layers are shared between parent and child nodes. Additional layers are introduced right after the second MLP unit to make use of the local feature response. A 1000 dimensional vector is produced to represent each image for MMC clustering. All other network parameter settings, weights initialization and learning policy strictly follow the settings provided by NIN [5].

Considering that most CIFAR-100 image classes are included in the ImageNet image classes, we pre-train each NIN in the SS-HCNN under two setups to study the difference with and without prior knowledge of the target dataset CIFAR-100. Under the first setup, each NIN in the tree, namely SS-HCNN_ImageNet_NIN, is pre-trained by using the whole ImageNet dataset where the prior knowledge of the target dataset is used. Under the second setup, we remove 500 classes of ImageNet images that overlap (with same or similar types of objects) with the CIFAR-100 images and use the rest 500 class images (ImageNet-500) for model pre-training. The pre-trained model SS-HCNN_ImageNet500_NIN thus has little prior knowledge of the target datasets.

During the pre-training of NIN, the initial learning rate of each CNN in the tree hierarchy is set at 0.01 which is then decreased by a factor of 10 after every 10K iterations. The mini-batch size is set at 256, and each CNN is split to 3 clusters ($K = 3$) with a cluster splitting threshold of 0.3. As CIFAR images and ImageNet images have different resolutions, ImageNet images are first resized to 256 pixels along the shorter side from which a 224×224 patch is cropped randomly. As the ImageNet is a million-scale dataset, we further down-sample the cropped image patch to 32×32 pixels and then perform global contrast normalization and ZCA whitening within each mini-batch to overcome the memory and computational constraints as in [28].

Experimental Results: We compare the proposed SS-HCNN_ImageNet_NIN and SS-HCNN_ImageNet500_NIN with the the baseline NIN [5] and the state-of-the-art hierarchical deep CNN (HD-CNN) [17] which also uses NIN as the base CNN. Fig. 2 shows the Top-1 error rates, where the horizontal axis denotes different proportions of the labelled training samples that are used for the supervised training of the leaf-node CNNs. Take the 80% case as an example. It uses 80% of labelled training images of the CIFAR-100 dataset for the training of the category-level CNNs at leaf nodes and the rest 20% training images are not used. When annotations of all training images are used, the leaf-node CNN training becomes fully supervised as shown in the 100% case in the figure. It can be seen that the performance of all four methods drops when the proportion of the image annotations used decreases. On the other hand, the SS-HCNN_ImageNet_NIN trained using 60% of the labelled training images can achieve comparable error rate (32.9%) with the fully trained HD-CNN (32.6%) using all labelled training images. This shows that the proposed SS-HCNN approach can address the data annotation constraint effectively. Further, it can also be seen that the SS-HCNN_ImageNet500_NIN with little prior knowledge of the CIFAR-100 achieves slight lower performance as compared with SS-HCNN_ImageNet_NIN with prior knowledge, but it still outperforms the baseline NIN and HD-CNN clearly.

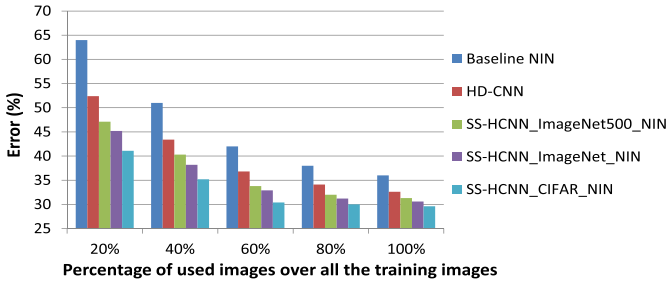

Fig. 2. Error rates (%) when different proportions of labelled training images are used (evaluated over the CIFAR-100): SS-HCNN_ImageNet500_NIN: SS-HCNN using the ImageNet-500 in NIN pre-training; SS-HCNN_ImageNet_NIN: SS-HCNN using the whole ImageNet in NIN pre-training; SS-HCNN_CIFAR_NIN: SS-HCNN using the CIFAR in NIN pre-training.

We also evaluate the fully supervised SS-HCNN that is trained by using all labelled training images, and compare it with other fully supervised CNN models. Table I shows experimental results. It can be seen that both fully trained SS-HCNN_ImageNet_NIN and SS-HCNN_ImageNet500_NIN achieve lower testing errors of 30.62% andd 31.30%, which outperform the state-of-the-art HD-CNN [17] and DDN [18] by 0.3%-2%.

Discussion: We study several key SS-HCNN training parameters and processes that are involved in the image hierarchy generation, cluster splitting and leaf CNN voting. In particular, one key parameter is K as described in Section 3.2 which controls how many child clusters a parent cluster is split in the hierarchical CNN tree. Another key parameter is the cluster splitting threshold that controls the cluster splitting by comparing it with the computed metric score d as defined in Eq. 5. Beyond these two key parameters, we also design a voting based image scoring technique as described in Section 3.5 that classifies images by integrating the output of multiple leaf-node CNNs. For the clarity of presentation and ease of understanding, we study these parameters and processes by using the 60% labelled images case where the SS-HCNN achieves comparable error rate with the fully trained HD-CNN as shown in Fig. 2.

We investigate the parameters K and splitting threshold by grid search where parameter K is set at $2, 3, 4, 5, 6, 7, 8$ and meanwhile the cluster splitting threshold changes from 0.1 to 1 with a step of 0.1. Fig. 3 shows experimental results. As Fig. 3 shows, the best classification result is obtained with $K = 3$ clusters under a threshold value of 0.3. It can also be observed that a larger number of clusters require

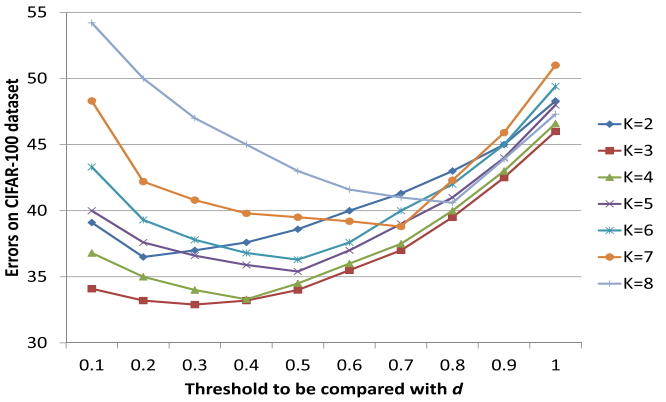

Fig. 3. Error rates (%) against different number of clusters and cluster splitting thresholds on the CIFAR-100 dataset.

TABLE I
ERRORS (%) ON THE CIFAR-100 DATASET

Method	Error
NIN	35.68
DSN [6]	34.68
CIFAR100-NIN	34.26
dasNet [7]	33.78
HD-CNN [17]	32.62
DDN [18]	31.65
SS-HCNN_ImageNet500_NIN	31.30
SS-HCNN_ImageNet_NIN	30.62
SS-HCNN_CIFAR_NIN	29.64

a larger threshold to achieve the optimal error rate, mainly because larger thresholds can offset the over-splitting effect as introduced by larger number of clusters. On the other hand, a smaller threshold and larger K can easily increase the over-splitting risk by splitting a cluster into a large number of child clusters. It also introduces more computations as the system needs to train a larger number of cluter-level and leaf-level CNNs. We therefore fix the number of clusters $K = 3$ and the cluster splitting threshold at 0.3 for the CIFAR-100 dataset as described in the previous subsection. Under this setting, we observed that there are totally 36 nodes in the tree with a depth of three layers, and the number of image categories within each leaf-node cluster ranges from 1 to 8.

We also study the voting based image scoring technique as described in Section 3.5. We compare it with the traditional hierarchical tree traversal method that determines the cluster based on the highest score only. Experimental results show that the proposed voting strategy obtains an error rate of 32.9% which is 1.1% lower than 34.0% as achieved by using the traditional tree traversal method.

Further to make a fair comparison with HD-CNN [17] as well as other state-of-the-art techniques, we also used a held-out training set (10K images as used in [17]) with label annotations from CIFAR to pre-train the NIN, and then use the pre-trained NIN to perform MMC clustering to generate coarse categories. The newly trained model is named by SS-HCNN_CIFAR_NIN as shown in Fig. 2 and Table I. It can be seen that the SS-HCNN_CIFAR_NIN (using CIFAR pre-trained NIN) clearly outperforms the model in [17] (using CIFAR pre-trained NIN) due to our proposed hierarchical learning framework. At the same time, the SS-HCNN_CIFAR_NIN also outperforms the SS-HCNN_ImageNet_NIN (using ImageNet pre-trained NIN). The better performance can be explained by the CIFAR pre-trained NIN which is supervised and has better representative capability for the CIFAR images as compared with the ImageNet pretrained NIN.

B. ImageNet

Experiment Setup: For the ImageNet, we adopt the VGG-16 [2] as the network structure at each node of the SS-HCNN. The layers from conv1_1 to pool4 are shared between parent and child nodes, and the remaining layers are used as rear discriminative layers for image classification. All other network parameter settings and learning policy follow the settings provided by VGG-16. We use the VGG model pre-trained on the CIFAR-100 dataset, and then fine tune each node CNN by using images in the ImageNet (or ImageNet-500) dataset as described in Section 3.2 (namely SS-HCNN_CIFAR_VGG).

Similar to the experiments for the CIFAR-100 dataset, we conduct two groups of experiments on the whole ImageNet dataset and ImageNet-500 dataset respectively, to observe the influence with and without prior knowledge of the target dataset on the results. The minibatch size is also set at 256. As the size of feature maps after conv5_3 of VGG-16 is reduced to $1/16$ of the original image size, the CIFAR image (32×32 pixels) after conv5_3 becomes 2×2 pixels. The 2×2 feature map then goes through the pool5, fc6, fc7 and fc8 and becomes a 100-dimensional softmax output vector. In our system, we use the fc7 output, a 4096 dimensional vector, for MMC clustering as it captures richer information. During fine-tuning, the fc8 output is changed to the number of clusters (K=4) and categories for the cluster-level and category-level CNN training. The results on the ImageNet are derived via single scale central cropping (central 224×224 patch is cropped).

Different amounts of labelled training images are employed to train the leaf-node CNNs. The image hierarchy is set with $K = 4$ clusters at each node and the cluster splitting threshold is set at 0.3. The initial learning rate for each node CNN is set at 0.001, and it is decreased by a factor of 10 every 4K iterations.

Experimental Results: We compare the SS-HCNN_CIFAR_VGG with the baseline VGG [2] and the hierarchical deep CNN (HD-CNN) [17]. Fig. 4 shows Top-1 error rates on the ImageNet validation when different amounts of labelled training images are used. As Fig. 4 shows, the error rates of all three methods drop as the proportion of the used image annotations increases, but the SS-HCNN_CIFAR_VGG has the least error rate drop, followed by the HD-CNN and the baseline VGG. On the other hand, it can be observed that the SS-HCNN_CIFAR_VGG trained using 60% of labelled training images can achieve comparable error rate (24.1%) with the fully trained HD-CNN (23.7%) using all labelled training images. This again demonstrates that the proposed

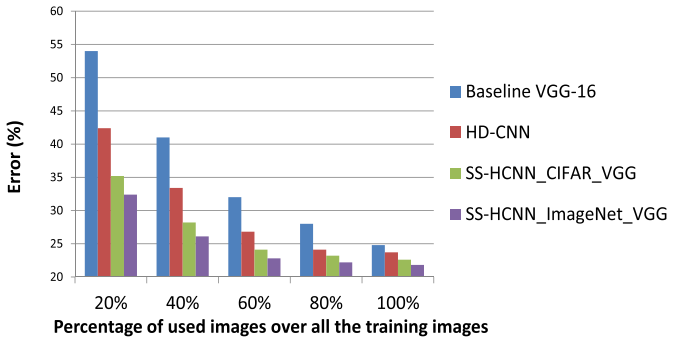

Fig. 4. Error rates (%) when different proportions of labelled training images are used (evaluated over the whole ImageNet validation set): SS-HCNN_CIFAR_VGG: SS-HCNN using CIFAR pre-trained VGG; SS-HCNN_ImageNet_VGG: SS-HCNN using ImageNet pre-trained VGG.

TABLE II
ERROR RATES (%) OF DIFFERENT FULLY TRAINED METHODS USING ALL THE TRAINING IMAGES ON THE IMAGENET VALIDATION SET

Method	Top-1	Top-5
GoogLeNet	N/A	7.9
Baseline VGG-16-layer	24.79	7.50
VGG-19-layer	24.8	7.5
VGG-16-layer+VGG-19-layer	24.0	7.1
HD-CNN	23.69	6.76
SS-HCNN_CIFAR_VGG	22.6	5.7
SS-HCNN_ImageNet_VGG	21.8	4.8

SS-HCNN approach can address the data annotation and uneven data separability constraints effectively.

We also compare the fully supervised SS-HCNN trained using all annotated images with other CNN models including the GoogLeNet [29], baseline VGG-16 [2], VGG-19 layer network [2], dense VGG-16-layer+VGG-19-layer [17] and HD-CNN [17] which are also fully trained by using all labelled training images. Table II shows experimental results. The VGG model based results are taken from Table IV of the HD-CNN. They are derived via dense evaluation over three scales 256, 384, 512 and better than the single scale evaluation as reported in [2]. It can be seen that the SS-HCNN obtains the lowest top-1 and top-5 error rates among all methods. Further, it is also observed that the SS-HCNN_ImageNet_VGG achieves better performance than SS-HCNN_CIFAR_VGG with the similar reason as discussed for the CIFAR experiments.

The evaluations have also been performed over the newly formed ImageNet-500 dataset. Fig. 5 shows experimental results. As Fig. 5 shows, the SS-HCNN_CIFAR_VGG (using CIFAR-100 in VGG pre-training) performs better than the baseline VGG-16 and HD-CNN consistently, demonstrating the advantage of the proposed SS-HCNN. In addition, the performance is slightly lower as compared with the evaluation over the whole ImageNet as shown in Fig. 4 (0.3%-1.8% when different proportions of training images are used) due to the overlap between the CIFAR-100 and the ImageNet.

Discussion: Similar to the CIFAR-100 dataset, we study the cluster splitting number K, the splitting threshold and the voting based image scoring for the ImageNet dataset. For the

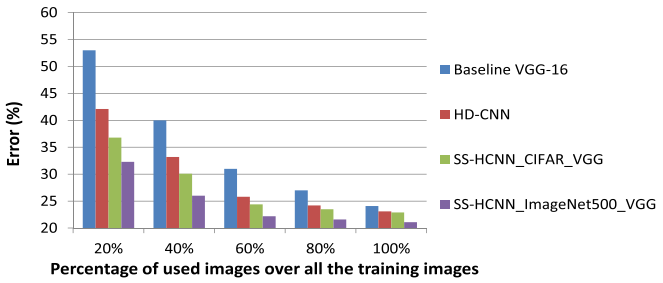

Fig. 5. Error rates (%) when different proportions of labelled training images are used (evaluated over the ImageNet-500 validation set): SS-HCNN_CIFAR_VGG: SS-HCNN using the CIFAR-100 in VGG pre-training; SS-HCNN_ImageNet500_VGG: SS-HCNN using the ImageNet-500 in VGG pre-training.

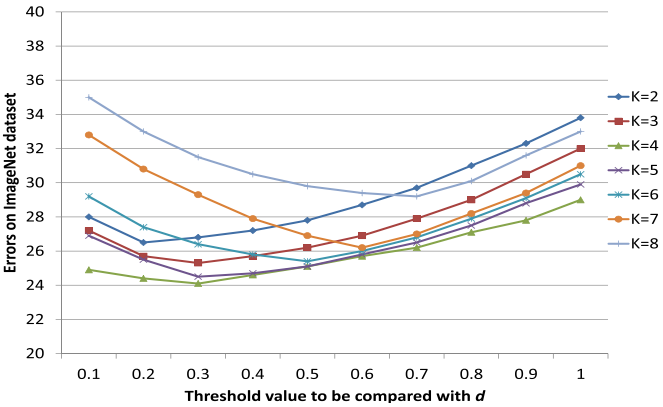

Fig. 6. Error rates (%) against different numbers of clusters and cluster splitting thresholds on the ImageNet validation set.

clarity of presentation and ease of understanding, we similarly use the 60% labelled images case where the SS-HCNN achieves comparable error rate with the fully trained HD-CNN as shown in Fig. 4.

We first investigate the parameters K and splitting threshold by grid search where parameter K is set at $2, 3, 4, 5, 6, 7, 8$ and meanwhile the cluster splitting threshold changes from 0.1 to 1 with a step of 0.1. Fig. 6 shows experimental results. As Fig. 6 shows, the lowest error rate is obtained with $K = 4$ clusters under a threshold value of 0.3. Similar to the CIFAR-100 dataset, it can be observed that a larger number of clusters require a larger threshold to achieve the optimal error rate. On the other hand, a larger optimal cluster number K is observed on the ImageNet dataset because the ImageNet data has a larger number of image categories and also a larger number of images within each image category. We therefore fix the number of clusters K at 4 and the cluster splitting threshold to be 0.3 as described in the previous subsections. Under this setting, it is observed there are totally 136 nodes in the tree with a depth of four, and the category number in each leaf node ranges from 5 to 20.

We also study the voting based image scoring technique and compare it with the traditional hierarchical tree traversal method. Experimental results show that the proposed voting strategy obtains 24.1% error rate which is 1.3% lower than the

TABLE III
COMPARISON OF MEMORY FOOTPRINT (MB) AND TESTING TIME (SECONDS) BETWEEN SS-HCNN AND OTHER NETWORKS ON CIFAR100 AND IMAGENET DATASETS. THE TESTING MINI-BATCH SIZE IS 50

Dataset	Models	Memory	Testing time
CIFAR100	Baseline NIN	188	0.04
	HD-CNN	286	0.1
	SS-HCNN	368	0.16
ImageNet	Baseline VGG-16	4134	1.04
	HD-CNN	6863	5.28
	SS-HCNN	8672	5.68

25.4% as achieved by the traditional hierarchical tree traversal method.

Similar to the experiments for the CIFAR dataset, we also follow the work [17] and use 100K held-out training images from the ImageNet to pre-train the VGG and then use the pre-trained VGG to perform MMC clustering to generate coarse categories. The newly trained model is named by SS-HCNN_ImageNet_VGG as shown in Table II and Fig. 4, and SS-HCNN_ImageNet500_VGG in Fig. 5. It can be seen that the SS-HCNN_ImageNet_VGG (or SS-HCNN_ImageNet500_VGG) clearly outperforms the model in [17] (using ImageNet pre-trained VGG) as well as the SS-HCNN_CIFAR_VGG with similar reasons.

C. Efficiency

We study the memory footprint and computational efficiency of the proposed SS-HCNN and compare it with the baseline CNN and the HD-CNN [17]. Table III shows experimental results. It can be seen that SS-HCNN consumes more memory footprint and has slightly longer testing time than the baseline and HD-CNN, largely due to its deeper hierarchy structure. In addition, HD-CNN employs product quantization for parameter compression, whereas our SS-HCNN does not perform any parameter compression. The memory footprint of the SS-HCNN can be further reduced by adopting similar parameter compression techniques.

We have also studied the Wall clock time of the SS-HCNN. For the SS-HCNN trained on ImageNet which contains 136 nodes and 5 to 20 image categories within each leaf-node cluster, it is found that fine-tuning the VGG at the root node takes around 48 hours and fine-tuning the VGG in each node of the following four levels takes an average of 11 hours, 4 hours, 2 hours and 1 hour, respectively. The whole SS-HCNN can be trained in around 3 days as the child-node VGGs at the same level can be trained in parallel and the base layers (Conv1 to Pool4) of the child-node VGGs are inherited from their parent VGG which require no further training.

For the computational complexity, it is noted that a VGG-16 model has around 15 billion flops (multiply-adds) [3]. As our SS-HCNN shares the conv1 to pool4 layers (between parent and child nodes) which takes around 88% of the total flops, the feature maps for these shared layers in the child nodes can be inherited from their parent node directly and the corresponding flops are saved accordingly. Therefore, the SS-HCNN with 136 nodes (VGGs) for the ImageNet will have around $(1-88\%)\times 135\times 15+1\times 15=258$ billion flops in the training process. During the testing stage, the proposed voting based image scoring method requires to traverse 1 (best case) or at most 2 (worst case) nodes for a parent node at each level. The flops therefore become $15\times(1+2\times 0.12+2^2\times 0.12+2^3\times 0.12+2^4\times 0.12)=69$ billion flops in the worst case, and $15\times(1+1\times 0.12+1\times 0.12+1\times 0.12+1\times 0.12)=22$ billion flops in the best case.

V. CONCLUSION

We present a semi-supervised hierarchical CNN (SS-HCNN) framework to solve the data annotation constraint and uneven data separability problem. The SS-HCNN identifies image hierarchy using a newly designed large-scale MMC technique, and groups images into different visually compact clusters at different hierarchical levels. A stage-wise training strategy is developed to train the SS-HCNN, where cluster-level CNNs at parent nodes are first trained based on the generated cluster labels in an unsupervised manner, and category-level CNNs at leaf nodes can then be trained by using a small amount of labelled image annotations. A voting based image scoring technique is designed to classify each image. Experiments on the CIFAR-100 and ImageNet datasets show that the proposed SS-HCNN can relieve the data annotation constraint and uneven data separability challenge effectively.

REFERENCES

[1] A. Krizhevsky, I. Sutskever, and G. E. Hinton, "ImageNet classification with deep convolutional neural networks," in *Proc. Adv. Neural Inf. Process. Syst.*, 2012, pp. 1097–1105.
[2] K. Simonyan and A. Zisserman. (2014). "Very deep convolutional networks for large-scale image recognition." [Online]. Available: https://arxiv.org/abs/1409.1556
[3] K. He, X. Zhang, S. Ren, and J. Sun. (2015). "Deep residual learning for image recognition." [Online]. Available: https://arxiv.org/abs/1512.03385
[4] Z. Dong, Y. Wu, M. Pei, and Y. Jia, "Vehicle type classification using a semisupervised convolutional neural network," *IEEE Trans. Intell. Transp. Syst.*, vol. 16, no. 4, pp. 2247–2256, Aug. 2015.
[5] M. Lin, Q. Chen, and S. Yan. (2013). "Network in network." [Online]. Available: https://arxiv.org/abs/1312.4400
[6] C.-Y. Lee, S. Xie, P. Gallagher, Z. Zhang, and Z. Tu, "Deeply-supervised nets," in *Proc. AISTATS*, vol. 2, 2015, p. 6.
[7] M. F. Stollenga, J. Masci, F. Gomez, and J. Schmidhuber, "Deep networks with internal selective attention through feedback connections," in *Proc. Adv. Neural Inf. Process. Syst.*, 2014, pp. 3545–3553.
[8] D. C. Ciresan, U. Meier, J. Masci, and J. Schmidhuber, "Flexible, high performance convolutional neural networks for image classification," in *Proc. Int. Joint Conf. Artif. Intell. (IJCAI)*, vol. 22, 2011, pp. 1237–1242.
[9] J. Weston, F. Ratle, H. Mobahi, and R. Collobert, "Deep learning via semi-supervised embedding," in *Neural Networks: Tricks of the Trade*. Springer, 2012, pp. 639–655.
[10] R. Johnson and T. Zhang, "Supervised and semi-supervised text categorization using LSTM for region embeddings," in *Proc. 33rd Int. Conf. Mach. Learn.*, 2016, pp. 526–534.
[11] R. Johnson and T. Zhang, "Semi-supervised convolutional neural networks for text categorization via region embedding," in *Proc. Adv. Neural Inf. Process. Syst.*, 2015, pp. 919–927.
[12] G. Papandreou, L.-C. Chen, K. P. Murphy, and A. L. Yuille, "Weakly and semi-supervised learning of a deep convolutional network for semantic image segmentation," in *Proc. IEEE Int. Conf. Comput. Vis.*, Dec. 2015, pp. 1742–1750.
[13] P. Bojanowski and A. Joulin. (2017). "Unsupervised learning by predicting noise." [Online]. Available: https://arxiv.org/abs/1704.05310

[14] J. Deng *et al.*, "Large-scale object classification using label relation graphs," in *Proc. Eur. Conf. Comput. Vis. (ECCV)* Springer, 2014, pp. 48–64.
[15] T. Xiao, J. Zhang, K. Yang, Y. Peng, and Z. Zhang, "Error-driven incremental learning in deep convolutional neural network for large-scale image classification," in *Proc. 22nd ACM Int. Conf. Multimedia*, 2014, pp. 177–186.
[16] G. Hinton, O. Vinyals, and J. Dean. (2015). "Distilling the knowledge in a neural network." [Online]. Available: https://arxiv.org/abs/1503.02531
[17] Z. Yan *et al.*, "HD-CNN: Hierarchical deep convolutional neural networks for large scale visual recognition," in *Proc. Int. Conf. Comput. Vis. (ICCV)*, vol. 2, Dec. 2015, pp. 2740–2748.
[18] V. N. Murthy, V. Singh, T. Chen, R. Manmatha, and D. Comaniciu, "Deep decision network for multi-class image classification," in *Proc. IEEE Int. Conf. Comput. Vis. Pattern Recognit.*, Jun. 2016, pp. 2240–2248.
[19] K. Ahmed, M. H. Baig, and L. Torresani, "Network of experts for large-scale image categorization," in *Proc. 14th Eur. Conf. Comput. Vis.*, 2016, pp. 516–532.
[20] L. Xu, J. Neufeld, B. Larson, and D. Schuurmans, "Maximum margin clustering," in *Proc. Adv. Neural Inf. Process. Syst.*, 2004, pp. 1537–1544.
[21] J. Liu, T. Xia, J. Wang, Y. Yang, F. Zhou, and Y. Lin. (2016). "Fully convolutional attention networks for fine-grained recognition." [Online]. Available: https://arxiv.org/abs/1603.06765
[22] E. Gundogdu, E. S. Parıldı, B. Solmaz, V. Yücesoy, and A. Koç, "Deep learning-based fine-grained car make/model classification for visual surveillance," *Proc. SPIE*, vol. 10441, p. 104410J, Oct. 2017.
[23] J. Dong, Q. Chen, J. Feng, K. Jia, Z. Huang, and S. Yan, "Looking inside category: Subcategory-aware object recognition," *IEEE Trans. Circuits Syst. Video Technol.*, vol. 25, no. 8, pp. 1322–1334, Aug. 2015.
[24] K. Zhang, I. W. Tsang, and J. T. Kwok, "Maximum margin clustering made practical," *IEEE Trans. Neural Netw.*, vol. 20, no. 4, pp. 583–596, Apr. 2009.
[25] A. Krizhevsky and G. Hinton, "Learning multiple layers of features from tiny images," M.S. thesis, Dept. Comput. Sci., Univ. Toronto, Toronto, ON, Canada, 2009.
[26] J. Deng, W. Dong, R. Socher, L.-J. Li, K. Li, and L. Fei-Fei, "ImageNet: A large-scale hierarchical image database," in *Proc. IEEE Conf. Comput. Vis. Pattern Recognit. (CVPR)*, Jun. 2009, pp. 248–255.
[27] Y. Jia *et al.*, "Caffe: Convolutional architecture for fast feature embedding," in *Proc. 22nd ACM Int. Conf. Multimedia*, 2014, pp. 675–678.
[28] L. Huang, D. Yang, B. Lang, and J. Deng, "Decorrelated batch normalization," in *Proc. IEEE Conf. Comput. Vis. Pattern Recognit.*, Apr. 2018, pp. 791–800.
[29] C. Szegedy *et al.*, "Going deeper with convolutions," in *Proc. IEEE Conf. Comput. Vis. Pattern Recognit.*, Jun. 2015, pp. 1–9.

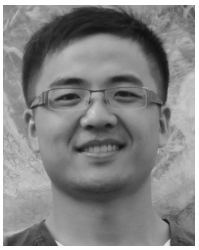

Tao Chen received the Ph.D. degree in information engineering from Nanyang Technological University, Singapore, in 2013. He was a Research Scientist at the Institute for Infocomm Research, A*STAR, Singapore, from 2013 to 2017, and a Senior Scientist at the Huawei Singapore Research Center from 2017 to 2018. He is currently a Professor with the School of Information Science and Technology, Fudan University, Shanghai, China. His main research interests include computer vision and machine learning.

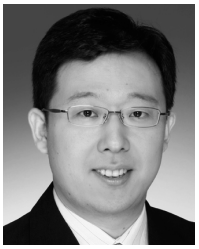

Shijian Lu received the Ph.D. degree in electrical and computer engineering from the National University of Singapore in 2005. He is currently an Assistant Professor with the School of Computer Science and Engineering, Nanyang Technological University, Singapore. His main research interests include document image analysis and understanding, computer vision, and pattern recognition.

Jiayuan Fan received the Ph.D. degree in information engineering from Nanyang Technological University, Singapore, in 2015. She is currently a Research Scientist at the Institute for Infocomm Research, A*STAR, Singapore. Her main research interests include computer vision, and image forensic analysis and application.